

Cutoff Frequency of a Homogeneous Optical Fiber with Arbitrary Cross Section

CHING-CHUAN SU

Abstract—Through an original derivation of the boundary conditions right at cutoff, the method of circular-harmonic expansion proposed by Goell to calculate propagation constants is extended to treat cutoff frequencies of homogeneous optical fibers with arbitrary cross sections in the rigorous vector form. This circular-harmonic method is also extended to the scalar form, from which the cutoff frequency can be obtained in a simpler way. Numerical results of cutoff frequencies of both the vector and the scalar forms are presented.

I. INTRODUCTION

TO CALCULATE the propagation constant of a homogeneous optical fiber with arbitrary cross section, several numerical methods have been proposed, such as the method of circular-harmonic expansion [1], [2], the extended boundary condition [3], [4], the generalized telegraphist's equation [5], and the method of surface integral equations [6], whereas, except for [6], few papers have discussed the calculation of cutoff frequencies of noncircular dielectric waveguides. Based on the scalar form of the extended boundary condition, Eges *et al.* [3] have presented some cutoff frequency data of such a structure, but no methods of extracting them were mentioned.

In this investigation, the boundary field-matching conditions right at cutoff are originally derived; thereupon, the aforementioned method of circular-harmonic expansion developed by Goell is extended to treat the cutoff frequencies of homogeneous optical fibers with arbitrary cross sections in the rigorous vector form. We also extend this circular-harmonic method to the scalar form, from which the cutoff frequency can be obtained in a simpler way, as discussed in Section II. Vectorial and scalar results of cutoff frequencies of elliptical and rectangular waveguides are presented in Section III.

II. FORMULATION

Consider a homogeneous dielectric cylinder of arbitrary cross section cladded by a homogeneous medium. Along such a structure, a time-harmonic electromagnetic field of angular frequency ω propagates with a propagation constant β in the axial (z) direction.

Manuscript received November 28, 1984; revised May 23, 1985.

The author was with the Department of Electrical Engineering, National Taiwan University, Taipei, Taiwan, Republic of China. He is now with the Department of Electrical Engineering, National Tsing Hua University, Hsinchu, Taiwan, R.O.C.

A. Vector Form

The propagation problem can be solved in the rigorous vector form via the axial components of the fields E_z and H_z , which are *real* quantities for guided modes and can be represented respectively in summations of the Bessel functions (or modified Bessel functions of the second kind) multiplied by angular phase factors as

$$E(r, \phi) = \operatorname{Re} \left\{ \sum_{m=0}^{\infty} a_m^s G_m^s(r) e^{-jm\phi} \right\} \quad (1)$$

and

$$H(r, \phi) = \operatorname{Re} \left\{ \sum_{m=0}^{\infty} j b_m^s G_m^s(r) e^{-jm\phi} \right\} \quad (2)$$

where $E = E_z$, $H = (\omega\mu_0/\beta)H_z$, $s = i$ (denoting the interior region) or e (denoting the exterior region), $G_m^i(r) = J_m(u)$, $G_m^e(r) = K_m(w)$, $u = (k_0^2\epsilon_i - \beta^2)^{1/2}r$, $w = (\beta^2 - k_0^2\epsilon_e)^{1/2}r$, k_0 denotes the free-space propagation constant, and a_m^i , a_m^e , b_m^i , and b_m^e are unknown complex coefficients. Note that a pure imaginary number j is introduced before b_m^s in (2) to simplify the following discussion. Once the axial components are obtained, other components can be deduced from them directly. Among the transverse components, those directed counterclockwise along the periphery of the cylinder can be given by

$$\begin{aligned} \frac{-j}{\beta} E_i(r, \phi) &= \frac{\partial H}{\partial n} - \frac{\partial E}{\partial l} \\ &= \operatorname{Re} \left\{ \frac{j}{k_0^2\epsilon_s - \beta^2} \sum_{m=0}^{\infty} G_m^s e^{-jm\phi} \right. \\ &\quad \left. \cdot \left[a_m^s \left(\cos \theta \frac{m}{r} - j \sin \theta \frac{G_m^{s'}}{G_m^s} \right) \right. \right. \\ &\quad \left. \left. + b_m^s \left(\cos \theta \frac{G_m^{s'}}{G_m^s} - j \sin \theta \frac{m}{r} \right) \right] \right\} \quad (3) \end{aligned}$$

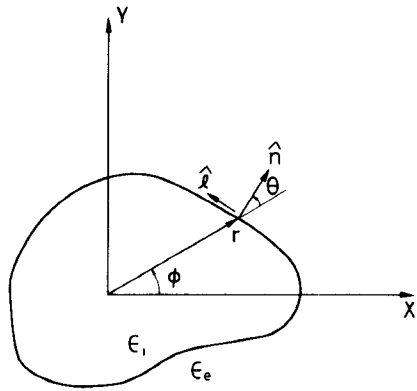


Fig. 1. The cross section of a homogeneous arbitrarily-shaped optical fiber.

and

$$\begin{aligned} j\omega\mu_0 H_l(r, \phi) &= \frac{\frac{k_0^2\epsilon_s}{\beta^2} \frac{\partial E}{\partial n} + \frac{\partial H}{\partial l}}{k_0^2\epsilon_s - \beta^2} \\ &= \operatorname{Re} \left\{ \frac{1}{k_0^2\epsilon_s - \beta^2} \sum_{m=0}^{\infty} G_m^s e^{-jm\phi} \right. \\ &\quad \cdot \left[a_m^s \left(\cos \theta \frac{G_m^{s'}}{G_m^s} - j \sin \theta \frac{m}{r} \right) \frac{k_0^2\epsilon_s}{\beta^2} \right. \\ &\quad \left. \left. + b_m^s \left(\cos \theta \frac{m}{r} - j \sin \theta \frac{G_m^{s'}}{G_m^s} \right) \right] \right\} \quad (4) \end{aligned}$$

where $G_m' = dJ_m(u)/dr$, $G_m'' = dK_m(w)/dr$, and $\partial/\partial n$ and $\partial/\partial l$ denote the derivatives in the \hat{n} and \hat{l} directions, respectively. Explicitly

$$\partial/\partial l = -\sin \theta \partial/\partial r + (\cos \theta/r) \partial/\partial \phi$$

and

$$\partial/\partial n = \cos \theta \partial/\partial r + (\sin \theta/r) \partial/\partial \phi$$

where θ denotes the angle between r and \hat{n} (see Fig. 1).

If one terminates the infinite summations after M terms and forces the four kinds of tangential fields of the two regions to be continuous at $N (= 2M)$ node points distributed around the periphery, one arrives at $4N$ simultaneous real equations with unknown variables being the real and the imaginary parts of a_m^i , b_m^i , a_m^e , and b_m^e . (Actually, due to the term of $\sin(m\phi)$ with $m=0$, the imaginary parts of a_0^s and the real parts of b_0^s are deleted and, accordingly, one of the node points is deleted.) Then, the propagation constants of guided modes can be determined by searching the roots of the determinant of the resultant matrix.

However, at the cutoff condition ($q (= \epsilon_e - \beta^2/k_0^2) \rightarrow 0$), special consideration should be taken for the exterior transverse fields since the vanishing denominators occur in (3) and (4) and the expansion functions $K_m(w)$ are singular themselves. The singularity of K_m at cutoff can be removed by retaining only their relative magnitudes (for each order of K_m) among the node points; that is, $K_m(w)$ is recognized as r^{-m} at cutoff.

The singularity due to the vanishing denominators can be removed by noticing the behavior of the modified Bessel functions with vanishing arguments. As q approaches zero from a negative value

$$K_0'(w)|_{w \rightarrow 0} = -1/r \quad (5a)$$

and

$$\frac{K'_m(w)}{K_m(w)} \Big|_{w \rightarrow 0} = -\frac{m}{r} + qrQ_m, \quad \text{for } m \geq 1 \quad (5b)$$

where

$$\begin{aligned} Q_m &= -k_0^2 \ln(\gamma_E w/2), \quad \text{for } m=1 \\ &= k_0^2/2(m-1), \quad \text{for } m > 1 \end{aligned}$$

and $\gamma_E (= 1.781 \dots)$ denotes Euler's constant whose numerical value will not be encountered in actual calculation. From (3)–(5), one can conclude the following: For the transverse fields remaining finite in the exterior region, it requires that

$$b_m^e = a_m^e + qf_m, \quad \text{for } m > 0 \quad (6)$$

and that a_0^e and b_0^e should vanish to the first order of q , where f_m are unknown complex quantities. Further, it is noted that the quantity of $\epsilon_e/(\beta/k_0)^2$ in (4) can be replaced by $(1+q/\epsilon_e)$, as q approaches zero. Then we obtain the representations of the exterior transverse fields along the peripheral direction at cutoff as

$$\begin{aligned} -\frac{jk_0^2}{\beta} E_l(r, \phi) &= \operatorname{Re} \left\{ -(a_0^e \sin \theta + jb_0^e \cos \theta)/(qr) \right. \\ &\quad \left. + \sum_{m=1}^{\infty} jK_m(w) e^{-jm\phi} \left[-f_m \frac{m}{r} e^{j\theta} + a_m^e r Q_m e^{-j\theta} \right] \right\} \quad (7) \end{aligned}$$

and

$$\begin{aligned} \frac{jk_0^2\omega\mu_0}{\beta^2} H_l(r, \phi) &= \operatorname{Re} \left\{ -(a_0^e \cos \theta - jb_0^e \sin \theta)/(qr) \right. \\ &\quad \left. + \sum_{m=1}^{\infty} K_m(w) e^{-jm\phi} \left[f_m \frac{m}{r} e^{j\theta} + a_m^e \left(r Q_m e^{-j\theta} - \frac{m}{r\epsilon_e} e^{j\theta} \right) \right] \right\}. \quad (8) \end{aligned}$$

Using (7) and (8) to represent E_l and H_l in the exterior region and applying the relation of $b_m^e = a_m^e$ (letting $q=0$ in (6)) to (2), one arrives at $4N$ simultaneous real equations with unknown variables being the real and the imaginary parts of a_m^i , b_m^i , a_m^e , and f_m (replacing notationally b_0^e with f_0), after the same point-matching procedure. Note that since Q_1 becomes infinite and a_1^e becomes zero accordingly, the quantity of $a_1^e Q_1$ is undetermined. In view of this, we replace the to-be-solved unknown a_1^e with $a_1^e Q_1$. Similarly, we replace the unknowns a_0^e and f_0 with a_0^e/q and f_0/q , respectively. Thereafter, the cutoff frequencies of guided modes are determined by searching the values of V which render the determinant of the resultant matrix vanishing, where $V (= k_0 [\tilde{A}(\epsilon_i - \epsilon_e)/\pi]^{1/2})$ denotes the normalized frequency and \tilde{A} denotes the cross-sectional area. Through such a normalized quantity, cutoff frequencies of guided modes are determined by knowing the ratio

ϵ_r between ϵ_i and ϵ_e ($\epsilon_r = \epsilon_i/\epsilon_e$), not necessarily by their respective values.

B. Scalar Form

In the case of $\epsilon_r \rightarrow 1$, the transverse fields and their gradients in any direction are continuous everywhere. Consequently, the propagation problem can be solved via a transverse field F in any (but fixed) direction of rectangular coordinates. This field and its derivative can be represented respectively by

$$F(r, \phi) = \operatorname{Re} \left\{ \sum_{m=0}^{\infty} a_m^s G_m^s e^{-jm\phi} \right\} \quad (9)$$

and

$$\frac{dF(r, \phi)}{dr} = \operatorname{Re} \left\{ \sum_{m=0}^{\infty} a_m^s G_m^s e^{-jm\phi} \left(\frac{G_m^{s'}}{G_m^s} \right) \right\} \quad (10)$$

where the notations a_m^s , G_m^s , and $G_m^{s'}$ are defined as before. Similarly, by terminating the infinite summations after M terms and forcing F and dF/dr to be continuous at $N (= 2M)$ points distributed around the periphery, one obtains $2N$ simultaneous real equations with unknown variables being the real and the imaginary parts of a_m^s and a_m^e . The resultant matrix can be used to find propagation constants as well as cutoff frequencies of guided modes. In the treatment of the cutoff frequency, the quantity of K'_m/K_m is taken as $-m/r$ (letting $q=0$ in (5)) and, again, only the relative magnitudes of $K_m(w)$ are retained.

C. Symmetry

If the cross section of the guiding structure possesses symmetry about some axis, there will be symmetry or antisymmetry in the corresponding field patterns. It can be shown that if E is symmetric about that axis, H will be antisymmetric, and vice versa. Due to the opposite symmetry between E and H , we refer to the symmetry types hereafter with respect to E . If E is symmetric (antisymmetric) about the x axis, the imaginary (real) parts of all the unknown coefficients (a_m^s , b_m^s , and f_m) are zero and the corresponding guided modes are referred to the symmetric (antisymmetric) modes hereafter. If the symmetric mode is further symmetric (antisymmetric) about the y axis or the antisymmetric mode is antisymmetric (symmetric) about the y axis, the summation index m in (1)–(4), (7), and (8) will run on even (odd) numbers and the corresponding modes are referred to the even (odd) modes. By exploiting the symmetry properties, the number of unknown coefficients and the number of node points will be reduced. In cases of two-fold symmetry, such as in elliptical or rectangular waveguides, it suffices to match the fields in one quadrant of the periphery. In the scalar form, the algorithm for symmetry is the same as that of the vector form. However, the physical interpretation is different, since the scalar form is formulated via a transverse field. It can be shown that, for a structure with two-fold symmetry, each scalar even (odd) mode is composed of two vectorial odd (even) modes, one symmetric and one antisymmetric.

To avoid confusion, we refer to the scalar symmetry type with respect to the corresponding symmetry in the vector form.

III. PROCEDURE AND RESULT

In the following calculation, we consider the elliptical and the rectangular waveguides which possess two-fold symmetry, and whose boundaries can be described by a superellipse [2] as

$$\left(\frac{r \cos \phi}{\gamma C} \right)^{2L} + \left(\frac{r \sin \phi}{C} \right)^{2L} = 1 \quad (11)$$

where γ denotes the aspect ratio such that $2C$ and $2\gamma C$ are, respectively, the lengths of the minor and the major axes, $L=1$ corresponds to an ellipse, and $L=\infty$ corresponds to a rectangle.

In our calculation, it is found that the calculated results depend on how the node points are chosen, especially when the aspect ratio becomes large. The results presented here correspond to those node points equiangularly distributed around the periphery; namely, the azimuthal angle of node point I is given by

$$\phi(I) = \frac{\pi}{2} \frac{I-0.5}{N}, \quad I=1, 2, \dots, N. \quad (12)$$

For the even modes, where the summations include the term of $\sin(m\phi)$ with $m=0$, two equations (one in (1) or (2) and the other in (3) or (4), depending on the modes being symmetric or antisymmetric) corresponding to the point of $I=1$ were deleted.

In general, one has to solve a $4N \times 4N$ matrix for the vector form just as was done in [1]. However, some of the computation can be saved if one first expresses explicitly a_m^s and b_m^s in terms of a_m^e from (1) and (2), respectively (by solving associated $N \times N$ matrices), and then substitutes these explicit relations in (3) and (4). Thereafter, one arrives at a $2N \times 2N$ matrix equation with unknowns being a_m^e and f_m . It can be shown that the total computation effort is about one-half that of solving a $4N \times 4N$ matrix equation directly. This time-saving procedure holds for the calculation of propagation constants.

The calculated cutoff frequencies of both the vector and the scalar forms are shown in Tables I and II for the elliptical and rectangular waveguides, respectively, where the modes designated by SE (AE) correspond to the symmetric (antisymmetric) even modes and those by SO (AO) correspond to the symmetric (antisymmetric) odd modes. The scalar data from [3] are also listed for comparison. It is found that most of their data are higher than ours. By further checking their data of circular waveguides, where exact solutions are available, we conclude that the cutoff data in [3] are not right at cutoff but just near it. Comparing Tables I and II, it is found that, for the modes shown, the cutoff frequencies of the elliptical waveguides are higher than those of the rectangular waveguides with the same aspect ratio and cross-sectional area.

Previously, it has been found that the elliptical [7] and

TABLE I
NORMALIZED CUTOFF FREQUENCY OF AN ELLIPTICAL WAVEGUIDE

MODE	$\epsilon_r = 2.25$		$\epsilon_r = 1.0404$		$\epsilon_r \rightarrow 1$	
	$\gamma=1.5$	$\gamma=2$	$\gamma=1.5$	$\gamma=2$	$\gamma=1.5$	$\gamma=2$
SE ₁	2.294	2.241	2.201	2.132	2.193 (2.23)*	2.084 (2.13)
AE ₁	2.389	2.399	2.206	2.139		
SE ₂	2.976	3.233	2.696	2.954	2.686 (2.77)	2.935 (2.98)
AE ₂	2.896	3.090	2.692	2.947		
SO ₂	3.408	3.127	3.355	3.126	3.351 (3.42)	3.104 (3.20)
AO ₂	3.483	3.300	3.360	3.135		
SO ₃	4.183	4.379	3.912	4.053	3.898 (3.89)	3.976 (4.09)
AO ₃	4.043	4.116	3.905	4.042		
SO ₄	4.576	5.014	4.459	4.984	4.457 (4.54)	4.982 (5.11)
AO ₄	4.646	5.126	4.462	4.988		

*The parenthesized data in Tables I and II are taken from [3]; however, due to the different definitions of normalized frequency, they are multiplied by a factor of $\pi\sqrt{\gamma}$ to conform our definition pertaining to cross-sectional area.

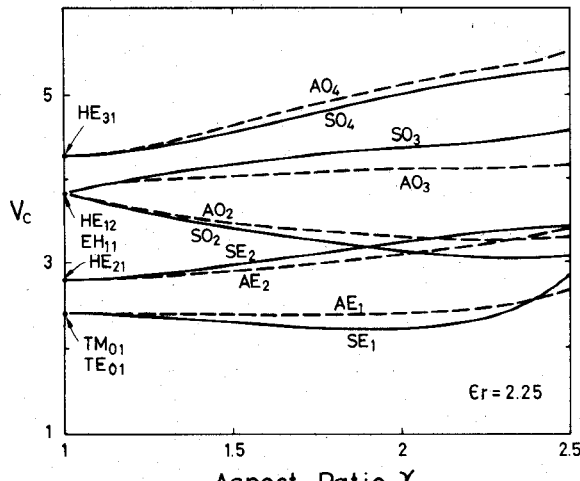
TABLE II
NORMALIZED CUTOFF FREQUENCY OF A RECTANGULAR WAVEGUIDE

MODE	$\epsilon_r = 2.25$			$\epsilon_r = 1.0404$			$\epsilon_r \rightarrow 1$		
	$\gamma=1$	$\gamma=1.5$	$\gamma=2$	$\gamma=1$	$\gamma=1.5$	$\gamma=2$	$\gamma=1$	$\gamma=1.5$	$\gamma=2$
SE ₁	2.097	2.026	1.988	2.143	1.953	1.857	2.137	1.929	1.849 (1.87)
AE ₁	2.176	2.094	2.096	2.146	1.953	1.860			1.849
SE ₂	2.592	2.754	2.987	2.173	2.443	2.715	2.137	2.408	2.704 (2.67)
AE ₂	2.327	2.519	2.745	2.161	2.436	2.705			2.704
SO ₂	3.286	3.032	2.838	3.237	3.044	2.838	3.196	3.011	2.836 (2.84)
AO ₂	3.286	3.098	2.917	3.237	3.045	2.841			2.836
SO ₃	3.425	3.648	3.855	3.366	3.318	3.487	3.325	3.220	3.471 (3.42)
AO ₃	3.425	3.422	3.594	3.366	3.311	3.477			3.471
SO ₄	3.925	4.219	4.702	3.682	4.157	4.705	3.671	4.128	4.706 (4.80)
AO ₄	3.925	4.330	4.823	3.682	4.160	4.710			4.706

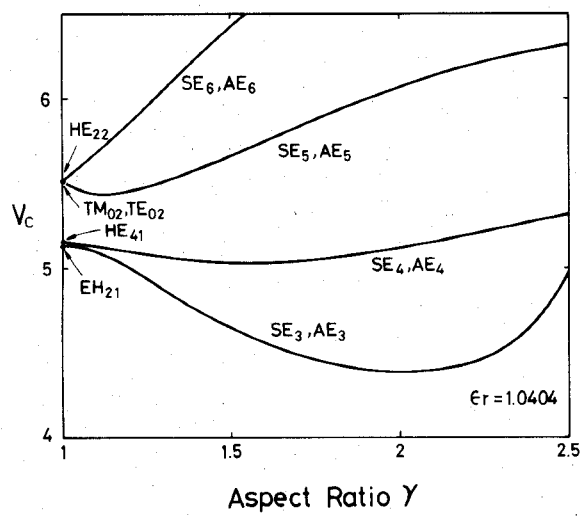
the rectangular [1] waveguides possess two fundamental modes which are never cutoff; indeed, we find that of the two lowest modes (the SO₁ and AO₁ modes), the cutoff frequencies cannot be found, namely, their cutoff values are both zero. The functional behavior of the cutoff frequencies of elliptical waveguides as the aspect ratio γ and the permittivity ratio ϵ_r are varying as shown in Figs. 2 and 3, respectively. It is found that, except for the TE and TM modes, each mode of a circular waveguide is split into two different modes (one symmetric and one antisymmetric) as the cross section becomes flatter. As to those elliptical modes evolving from the circular TE or TM modes, since their field patterns do not possess both symmetry and antisymmetry (about the x axis), no such splitting is observed; however, the degeneracy in the cutoff frequencies of the circular TE and TM modes is removed in an elliptical waveguide. Note that in the special case of the circular waveguide, the solutions of the present method correspond to the HE_{ml} modes with azimuthal mode number $m > 1$. For other circular modes, the cutoff frequencies are determined in another way [8] (which is specific to the circular waveguide), and one needs finer searching steps to locate the cutoff frequencies of elliptical modes which evolve from such circular modes, when γ is close to 1. From Fig. 2, one can also find that some of the cutoff

frequencies become higher and others become lower as the cross section becomes flatter. Yeh conjectured [7] that the cutoff frequencies of all modes (except the fundamental modes) become higher for a flatter (but same area) elliptical waveguide. Apparently, his early conjecture is not correct. However, his argument may be applied to waveguides of very large aspect ratios, in which case the portions near the ends of the major axes are expected to contribute little to the guiding mechanism. Fig. 3 illustrates that the splitting due to a nonunit aspect ratio increases as ϵ_r becomes larger, and vanishes again as ϵ_r approaches unity. Note that in the limit of $\epsilon_r \rightarrow 1$, the vectorial and scalar solutions do not agree very well, which is ascribed to the errors of calculation. For a smaller γ , this disagreement is seen to be smaller. The vanishing splitting as $\epsilon_r \rightarrow 1$ also exists in the propagation constants above cutoff; this explains why Eges *et al.* [3] failed to find two fundamental modes by employing a scalar formulation.

In the above calculation, we choose $N = 8$ and use a double precision. The aspect ratios are confined within 2.5; for larger aspect ratios, N should be increased to obtain satisfactory results. However, for such large aspect ratios, the increase of N is found to bring forth numerical instability. This instability seems due to the extraneous large variation of the numerical values of the Bessel or modified



(a)



(b)

Fig. 2. Relations of normalized cutoff frequency V_c versus aspect ratio γ of an elliptical waveguide with (a) $\epsilon_r = 2.25$ or (b) 1.0404. The discrepancies between the cutoff frequencies of symmetric and antisymmetric modes are too small to be shown in the drawing of (b).

Bessel functions among the node points when γ and N become large simultaneously.

IV. CONCLUSION

In this investigation, the boundary field-matching conditions right at cutoff are originally derived; thereupon, the vectorial method of circular-harmonic expansion is extended to treat the cutoff frequencies of homogeneous optical fibers with arbitrary cross sections. This circular-harmonic method is also extended to the scalar form, where the cutoff frequencies can be obtained in a simpler way.

From the calculated results, it is found that, except for the fundamental mode and the TE and TM modes, each mode of circular waveguide is split into two modes with different cutoff frequencies as the waveguide becomes elliptical. The dependences of cutoff frequency on the cross-sectional geometry and the permittivity ratio are illustrated.

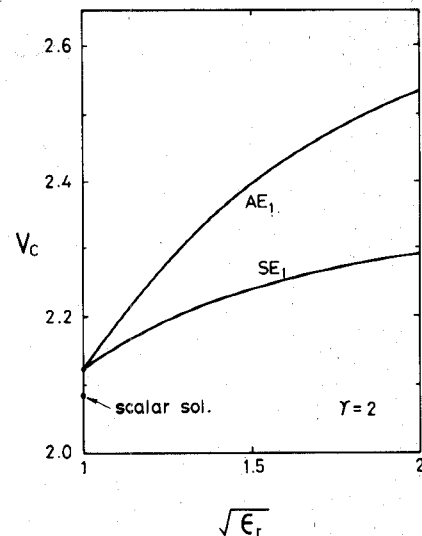


Fig. 3. Relations of normalized cutoff frequency V_c versus permittivity ratio ϵ_r for a symmetric and a corresponding antisymmetric modes of an elliptical waveguide.

REFERENCES

- [1] J. E. Goell, "A circular-harmonic computer analysis of rectangular dielectric waveguides," *Bell Syst. Tech. J.*, vol. 48, pp. 2133-2160, Sept. 1969.
- [2] A. L. Cullen, O. Özkan, and L. A. Jackson, "Point-matching technique for rectangular-cross-section dielectric rod," *Electron. Lett.*, vol. 7, pp. 497-499, Aug. 1971.
- [3] L. Egyes, P. Gianino, and P. Wintersteiner, "Modes of dielectric waveguides of arbitrary cross sectional shape," *J. Opt. Soc. Am.*, vol. 69, pp. 1226-1235, Sept. 1979.
- [4] N. Morita, "A method extending the boundary condition for analyzing guided modes of dielectric waveguides of arbitrary cross-sectional shape," *IEEE Trans. Microwave Theory Tech.*, vol. MTT-30, pp. 6-12, Jan. 1982.
- [5] H. Shinonaga and S. Kurazono, "Y dielectric waveguide for millimeter- and submillimeter-wave," *IEEE Trans. Microwave Theory Tech.*, vol. MTT-29, pp. 542-546, June 1981.
- [6] C.-C. Su, "A surface integral equations method for homogeneous optical fibers and coupled image lines of arbitrary cross-sections," *IEEE Trans. Microwave Theory Tech.*, this issue, pp. 1114-1119.
- [7] C. Yeh, "Elliptical dielectric waveguides," *J. Appl. Phys.*, vol. 33, pp. 3235-3243, Nov. 1962.
- [8] E. Snitzer, "Cylindrical dielectric waveguide modes," *J. Opt. Soc. Am.*, vol. 51, pp. 491-498, May 1961.

†



Ching-Chuan Su was born in Taiwan on October 2, 1955. He received the B.S., M.S., and Ph.D. degrees in electrical engineering from National Taiwan University in 1978, 1980, and 1985, respectively.

From 1980 to 1982, he was employed in an IC company, where he was responsible for the development of several MOS fabrication processes. In 1985, he joined the faculty of National Tsing Hua University, Hsinchu, Taiwan, where he currently serves as an Associate Professor in electrical engineering. His theoretical interests include bistability in nonlinear optics and numerical methods in dielectric waveguide, body scattering, and MOS device simulation.